Electronic Supplementary Information

Methods

Materials

Trifluoracetic acid (TFA), HPLC grade solvents and salts were from Chem-Supply (Australia), Sigma-Aldrich and Ajax Finechem. Hydrogen peroxide (30% w/w) was purchased from Chem-Supply (Australia). NADH disodium salt trihydrate was purchased from VWR International, LLC. Bovine liver catalase by Sigma-Aldrich. Kanamycin antibiotic was from Astral Scientific (Australia). Androstenedione was from TCI Chemicals and progesterone from Sigma-Aldrich. 16-α-hydroxyprogesterone was from Santa Cruz Biotechnology. Tris, dithiothreitol (DTT), lysozyme and isopropyl β-D-1-thiogalactopyranoside (IPTG) were from Astral Scientific (Australia). The *Escherichia coli* growth media and buffers composition is given in Table S1 Substrate, product and IS (internal standard) stock solutions were prepared in EtOH.

Buffers and Media

Table S1 Composition of buffers and growth media

Medium	**Constituents (L^{-1})**
LB broth	Bacto tryptone (10 g), Sodium chloride (5 g), Bacto yeast extract (5 g)
LB agar	Bacto yeast extract (5 g), Sodium chloride (5 g), Agar No. 1 (15 g), Bacto tryptone (10 g)
Super optimal broth (SOB)	NaCl (0.584 g), $MgSO_4$ (1.204 g), Tryptone (20 g), KCl (0.186 g), yeast extract (5 g), $MgCl_2$ (0.952 g)
Super optimal broth with catabolite repression (SOC)	20 mM glucose with SOB
Buffer T	1 mM DTT (dithiothreitol), 50 mM Tris-HCl buffer, pH 7.4
Binding buffer	20 mM Sodium phosphate (NaH_2PO_4 and Na_2HPO_4), 0.5 M NaCl, 30 mM imidazole, pH 7.4
Elution buffer	20 mM Sodium phosphate (NaH_2PO_4 and Na_2HPO_4), 0.5 M NaCl, 500 mM imidazole, pH 7.4
Trace elements	Na_2EDTA (20.1 g), $CaCl_2.H_2O$ (0.74 g), $FeCl_3.6H_2O$ (16.7 g), $CoCl_2.6H_2O$ (0.25 g), $MnSO_4.4H_2O$ (0.132 g), $CuSO_4.5H_2O$ (0.10 g), $ZnSO_4.7H_2O$ (0.18 g)

Production and purification of the T258E mutant and the wild-type form of CYP154

To perform protein expression and purification, the first step was to transform a pET28 plasmid which contained the CYP154C8 gene (WT or T258E mutant) into *E. coli* BL21 (DE3) competent cells (15 µL). The mixture was then kept on ice and incubated for 45 min and followed by heat shock at 42 ˚C for 45 s before it was cooled on ice for 2 min. Then, 250 µL of sterilized SOC media was added to the mixture and it was incubated at 37 ˚C at 180 rpm for 1 h. The bacteria were then spread on an LB agar plate containing kanamycin (30 mg L^{-1}); and incubated at 37 ˚C overnight (for ~20 h). Single colonies of the bacteria were introduced into four 500 mL volumes of LB broth containing kanamycin (30 mg L^{-1}) and the bacteria were incubated for ~8 h at 37 ˚C and 120 rpm. After this time, the temperature was reduced to 18 ˚C along with shaking to 95 rpm. Subsequently, 0.02% v/v benzyl alcohol and 2% v/v EtOH were added. Trace elements containing excess of iron (1.5 mL per 500 mL of media) were also added to the medium to aid heme incorporation (Table S1). After another 30 min incubation at 18 ˚C, 50 µL IPTG (isopropyl β-D-1-thiogalactopyranoside) was added to induce protein expression. The mixture was shaken at 95 rpm for a further 24 h at 18 ˚C. After incubating the culture for ~24 hours at 95 rpm and 18 ˚C, it was centrifuged (5000 g, 10 min, 4 ˚C) to collect the cell pellet. These cell pellets were then stored frozen at -20 ˚C. To resuspend the frozen cell pellet 200 ml of Tris buffer (pH 7.4, 50 mM) containing 1 mM DTT (dithiothreitol; this buffer is subsequently referred to as Buffer T, Table S1) was used. The cells were kept on ice and lysed by sonication (an Autotune CV334 converter probe at 70% amplitude and a VC505 Ultrasonic Processor, both from Sonics & Materials, USA) with manual stirring. To prevent overheating between each pulse of 20 s there was a 40 s interval. Soluble protein was collected by centrifugation at 39,000 g for 20 min at 4 ˚C to remove the cell debris.

The protein-containing supernatant was loaded onto a 5 mL HisTrap FF Crude histidine-tagged protein purification column (Cytiva). This column was equilibrated and washed with binding buffer (Table S1). After loading all the protein onto the column it was washed with binding buffer for about 8.5 mins. Elution buffer (Table S1) at a flow rate of 3 mL min^{-1} was used to elute the protein from the column. Red coloured protein fractions were collected, combined, and eluted down a Sephadex G-25 medium coarse grain desalting column to remove excess imidazole. The protein was then concentrated again using ultrafiltration (10 kDa exclusion membrane) and glycerol was added to a final concentration of 50 % v/v. Purified protein was stored at -20 ºC. The final protein concentration was determined using the extinction coefficient, ε_{418} = 130 mM^{-1} cm^{-1}. Before initiating subsequent experiments,

glycerol from P450 enzymes were removed using a 5 mL gel filtration column (PD-10, GE Healthcare).

P450 Carbon Monoxide Assay

A Cary 60 UV-Vis spectrophotometer (Agilent Technologies) was used to measure UV-Vis absorbance spectra. This was coupled to a Peltier unit to maintain the temperature at 30 ± 0.5 ˚C; and a quartz cuvette was used with a path length of 10 mm. The enzyme was diluted with Tris buffer (pH 7.4, 50 mM) to ≈ 6 - 10 μM. The UV-Vis spectrum of the P450 (500 μL) in Tris-HCl buffer was recorded from 250 to 700 nm. A few grains of sodium dithionite (< 1 mg) were added to the enzyme and its spectrum was used to baseline the instrument. Carbon monoxide (CO) was bubbled gently for about 10 s, through the solution to form the P450-CO adduct and its absorbance recorded to generate the ferrous-CO bound spectrum [1].

Substrate binding assays

Substrate binding typically causes the displacement of the heme-bound water to shift the heme iron from low-spin (LS) (Soret λ_{max} = ~418 nm) to high- spin (HS) (Soret λ_{max} = ~390 nm) [2]. Substrate binding may shift the spin-state fully or partially to HS [3]. The relevant P450 enzyme was diluted to ~ 1.5 – 2.2 μM with 50 mM Tris buffer (pH 7.4). Spin-state shift was measured by adding, 1 μL aliquots of a 100 mM substrate stock solution in EtOH to 500 μL of the P450 in Tris buffer (50 mM, pH 7.4). The UV-Vis absorbance spectrum was recorded after each addition, until there was no further shift of the spectrum. The UV-Vis spectrum was recorded from 700 nm to 250 nm. The fraction of the P450 enzyme in the high-spin state (% HS) was estimated ±5% by visually comparing the spectrum of the substrate-bound enzyme to a series of spectra of P450cam which show varying percentages of HS and LS enzyme [4].

For determining the binding affinity the purified P450 enzyme was diluted with Tris Buffer (50 mM, pH 7.4) to ≈ 1.5 μM. To 1 mL of protein, 1 μL aliquots of substrate from 10 μM to 100 mM substrate stock solutions in EtOH were then added using a 5 μL Hamilton syringe. Further 1 μL aliquots of substrate were added until the spectrum showed no further observable change. The resulting change in absorbance was recorded on a UV-Vis spectrophotometer (from 300–600 nm) until the peaks did not change upon further addition of substrate. Binding of a substrate induces a type I difference spectrum with a peak at ~390 nm and trough at ~420 nm [5]. Experiments were performed in triplicate. The peak-to-trough absorbance difference, ΔA (A_{peak} minus A_{trough}), was then plotted against substrate concentration. The data were fitted to the hyperbolic equation (Equation 1).

$$\Delta A = \frac{\Delta A_{max} \times [S]}{K_d + [S]} \quad (1)$$

Haem bleaching assay

In a cuvette 600 µL aliquot of CYP154C8 WT or the CYP154C8-T258E mutant solution (2 µM) in Tris buffer (50 mM, pH 7.4) containing 200 µM progesterone was used to baseline the UV-Vis spectrophotometer. Then, H_2O_2 (6, 20, 30, 40 or 60 mM) was added and the UV-Vis spectrum was recorded after 1 min. At 2 min intervals UV-Vis spectra was recorded and destruction of the haem prosthetic group was monitored.

***In vitro* H_2O_2 turnover**

Reaction mixtures contained 1 µM CYP154C8 (WT or T258E), 500 µM – 1 mM substrate from a 100 mM stock in EtOH, and 10 - 60 mM H_2O_2 in Tris buffer (50 mM, pH 7.4) in a total volume of 600 µL. Reaction mixtures were maintained for 4 hours in a shaking incubator (NB-205L benchtop shaking incubator, NBIOTEK) at 16 ˚C. Each reaction was performed in duplicate or triplicate. After 4 hours, 132 µL of reaction mixture were taken and quenched by mixing with 10 µL of 10 mg mL^{-1} bovine liver catalase to remove any leftover H_2O_2 from the reaction mixture [6, 7]. After quenching the reaction, 66 µL of MeCN was added to denature the enzyme followed by IS (*p*-cresol 2 µL from 20 mM stock) and trifluoroacetic acid (TFA) 2 µL. The mixture was centrifuged at 9000 rpm for 3 minutes to remove particulate matter prior to analysis by HPLC using a Shimadzu Prominence HPLC system. A Kinetex XB-C18 reversed-phase liquid chromatography column (250 × 4.6 mm, 5 µm) from Phenomenex with pore size of 100 Å, was used to perform high-performance liquid chromatography. A gradient: 20 – 95% MeCN in H_2O (with 0.1% TFA) at a rate of 1 mL min^{-1} over 30 minutes was used for elution. The detection wavelength was at 254 nm. Control reactions were performed with substrates (androstenedione or progesterone) in absence of H_2O_2 and P450 enzyme to assess enzymatic product formation.

In vitro turnovers were analyzed via GC-MS. Samples were prepared for GC-MS analysis by adding 4 µL of internal standard (20 mM *p*-cresol stock) in to 400 µL of the turnover mixture. This mixture was then extracted with 400 µL of EtOAc (thrice) and dried with anhydrous $MgSO_4$. Extracts were transferred to vials and analyzed via GC-MS. To perform Gas chromatography-mass spectrometry (GC-MS), GC-2010 Plus Gas chromatograph

(Shimadzu) with a GCMS-QP2010 SE mass spectrometer detector was used; with a 30 m SPB-5 column (0.25 mm i.d. and 0.25 μm thickness). An auto injector (AOC-20i Plus) and an auto sampler (AOC-20s Plus) were attached to this Gas chromatograph. The injection port and interface temperatures were set to 300 and 280 ˚C, respectively. The column/oven temperature was held at 70 ˚C for 1 minute before heating at 15 ˚C min^{-1} to 280 ˚C where it was held for 1 min before gradually increasing to 300 ˚C at a rate of 5 ˚C min^{-1}. When the column reached 300 ˚C, it was held for 10 min at this temperature.

Larger scale turnover reaction

Competent *E. coli* cells were transformed with the DNA vectors pET28 plasmid DNA containing CYP154C8 T258E mutant and plated onto LB_{kan}. One colony from the plate was taken and grown in 500 mL LB broth. The enzyme was expressed and purified by affinity chromatography and desalted according to the method described above. The protein from a 250 mL of growth was resuspeneded in 100 mL of Tris buffer (50 mM, pH 7.4) with 1 mM of progesterone or androstenedione in presence of 40 mM H_2O_2. The total volume of the reaction was 100 mL in a 500 mL flask for 2 hour and 1 mL aliquots were taken every 30 min to check the reaction by thin layer chromatography (TLC). Samples were prepared for TLC analysis by adding 5 μL of catalase to 200 μL of the turnover mixture. This mixture was then extracted with 300 μL of EtOAc (twice) and dried with anhydrous $MgSO_4$. TLC was then performed using a mixture of 60% EtOAc in Hexane as mobile phase to monitor the progress of the reaction. TLC were performed using precoated silica gel 60 F_{254} aluminum sheets (Merck) and viewed under UV light.

Isolation of Metabolites

All chemicals purchased from commercial suppliers were used without further purification, except for anhydrous solvents which were dried over molecular 3Å sieves. Column chromatography was performed using 20–63 μm grade silica gel. Thin layer chromatography was performed using aluminium sheets coated with silica gel 60 F_{254} purchased from Merck (Australia) and visualised using UV light (λ = 254 nm) and/or a $KMnO_4$ oxidizing stain ($KMnO_4$, K_2CO_3 and H_2O). All ^1H and ^{13}C NMR spectra were collected on a BRUKER AVANCE III 300 MHz FT-NMR spectrometer. All NMR experiments were performed at 25 °C. Samples were dissolved in $CDCl_3$, with the residual solvent peak used as the internal reference - $CDCl_3$: 7.26 (^1H) and 77.0 (^{13}C). NMR multiplicities are reported as broad (br), singlet (s), doublet (d), triplet (t), quartet (q) and multiplet (m). All J-values are rounded to the

nearest 0.1 Hz. High resolution mass spectrometry (HRMS) data was collected using an AB SCIEX TripleTOF 5600 mass spectrometer using a 95% MeOH in H_2O mobile phase containing 0.1% formic acid.

16α-hydroxy-progesterone

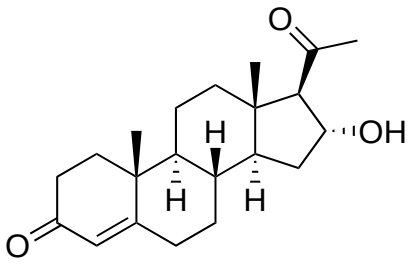

The aqueous media was extracted with EtOAc (3 x 115 mL) and the combined organic extracts were dried over anhydrous $MgSO_4$, filtered and concentrated *in vacuo*. The crude material was purified using flash chromatography on SiO_2 (60% - 80% EtOAc in *n*-hexane gradient) to afford the product as a white crystalline solid (7.6 mg). Data for 16α-hydroxy-progesterone matched that previously obtained in the literature.[8]

^{1}H NMR (300 MHz, $CDCl_3$) δ 5.74 (s, 1H), 4.86 – 4.81 (m, 1H), 2.54 (d, J = 6.5 Hz, 1H), 2.45 – 2.24 (m, 4H), 2.05 – 1.98 (m, 3H), 1.86 – 1.39 (m, 10H), 1.27 – 1.22 (m, 1H), 1.16 (s, 3H), 1.11 – 0.98 (m, 2H), 0.66 (s, 3H) ppm.
^{13}C NMR (75 MHz, $CDCl_3$) δ 208.9, 200.1, 171.4, 124.1, 73.5, 72.1, 53.8, 53.5, 45.0, 38.7, 38.6, 35.6, 35.2, 35.2, 33.9, 32.8, 31.8, 31.8, 20.7, 17.4, 14.6 ppm.

HRMS (ESI-TOF, *m/z*) for $C_{21}H_{30}O_3$ 331.2195 $[M + H]^+$, found 331.2865.

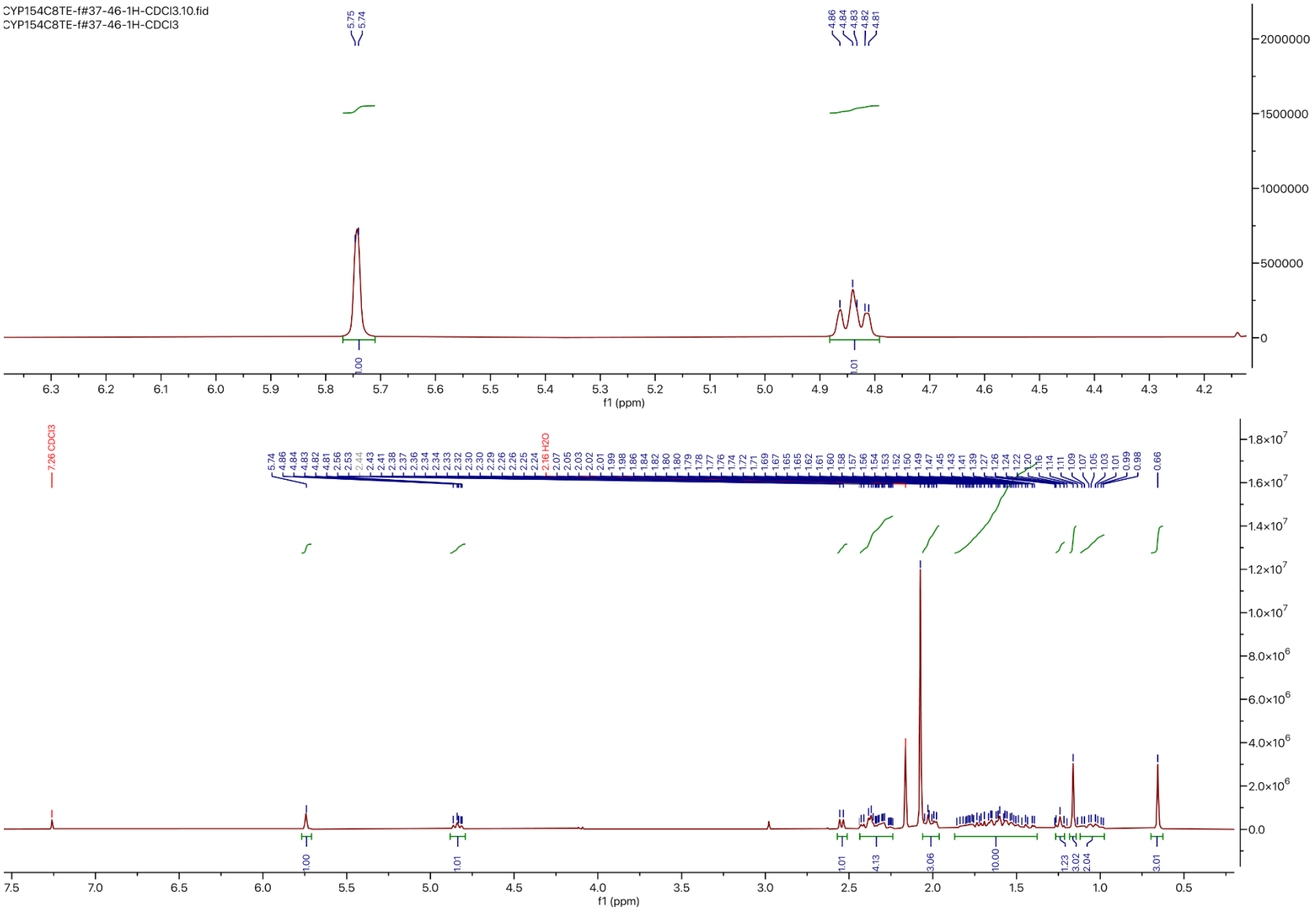
CYP154C8TE-f#37-46-1H-CDCl3.10.fid
CYP154C8TE-f#37-46-1H-CDCl3
5.75
5.74
4.86
4.84
4.83
4.82
4.81
2000000
1500000
1000000
500000
0
1.00
1.01
f1 (ppm)
7.26 CDCl3
2.16 H2O
0.66
1.8×10^7
1.6×10^7
1.4×10^7
1.2×10^7
1.0×10^7
8.0×10^6
6.0×10^6
4.0×10^6
2.0×10^6
0.0
1.00
1.01
1.01
4.13
3.06
10.00
1.23
3.02
2.04
3.01
f1 (ppm)

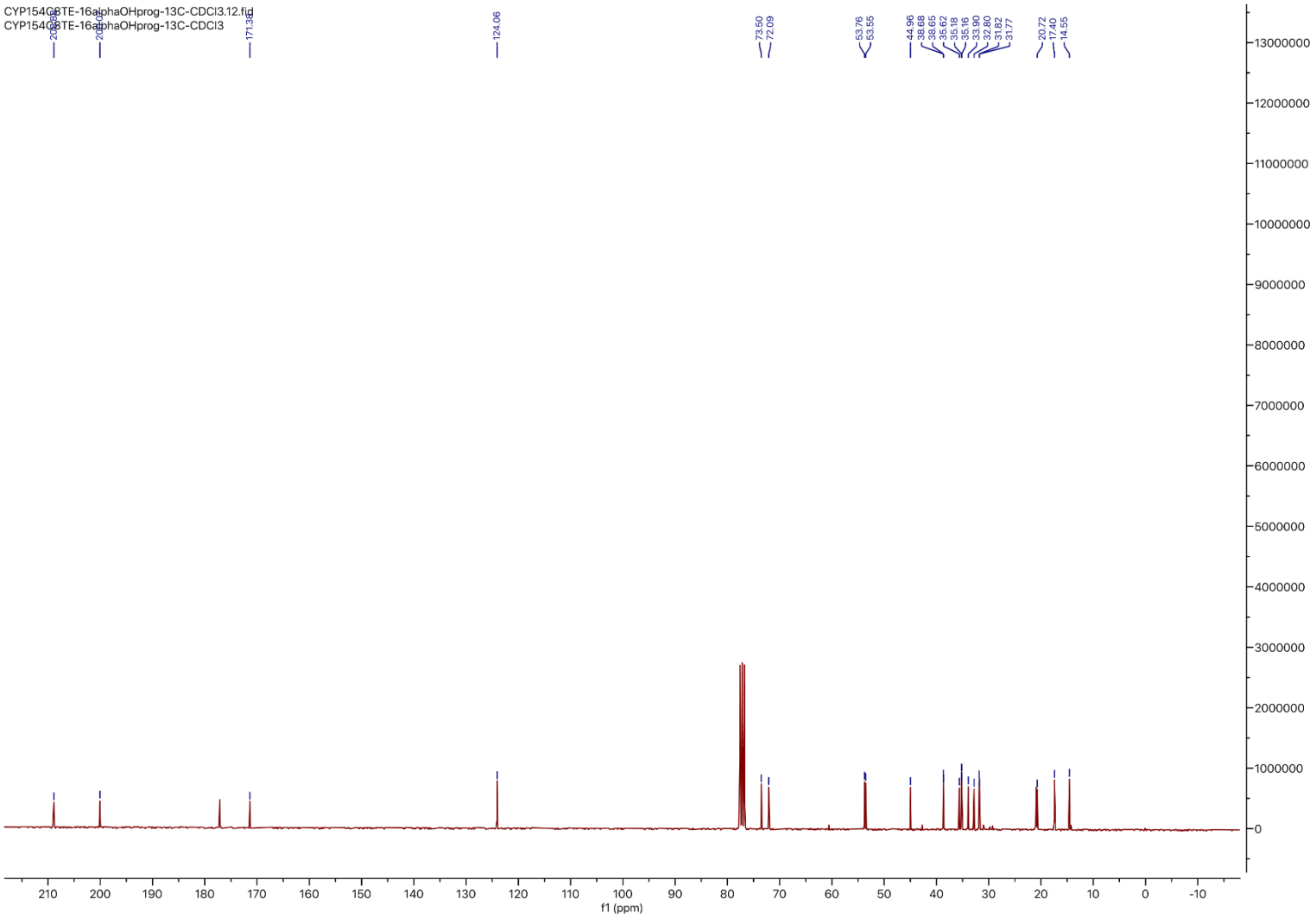
CYP154C8TE-16alphaOHprog-13C-CDCl3.12.fid
CYP154C8TE-16alphaOHprog-13C-CDCl3
208.68
208.05
171.38
124.06
73.50
72.09
53.76
53.55
44.96
38.68
38.65
35.62
35.18
35.16
33.90
32.80
31.82
31.77
20.72
17.40
14.55
13000000
12000000
11000000
10000000
9000000
8000000
7000000
6000000
5000000
4000000
3000000
2000000
1000000
0
210
200
190
180
170
160
150
140
130
120
110
100
90
80
70
60
50
40
30
20
10
0
-10
f1 (ppm)

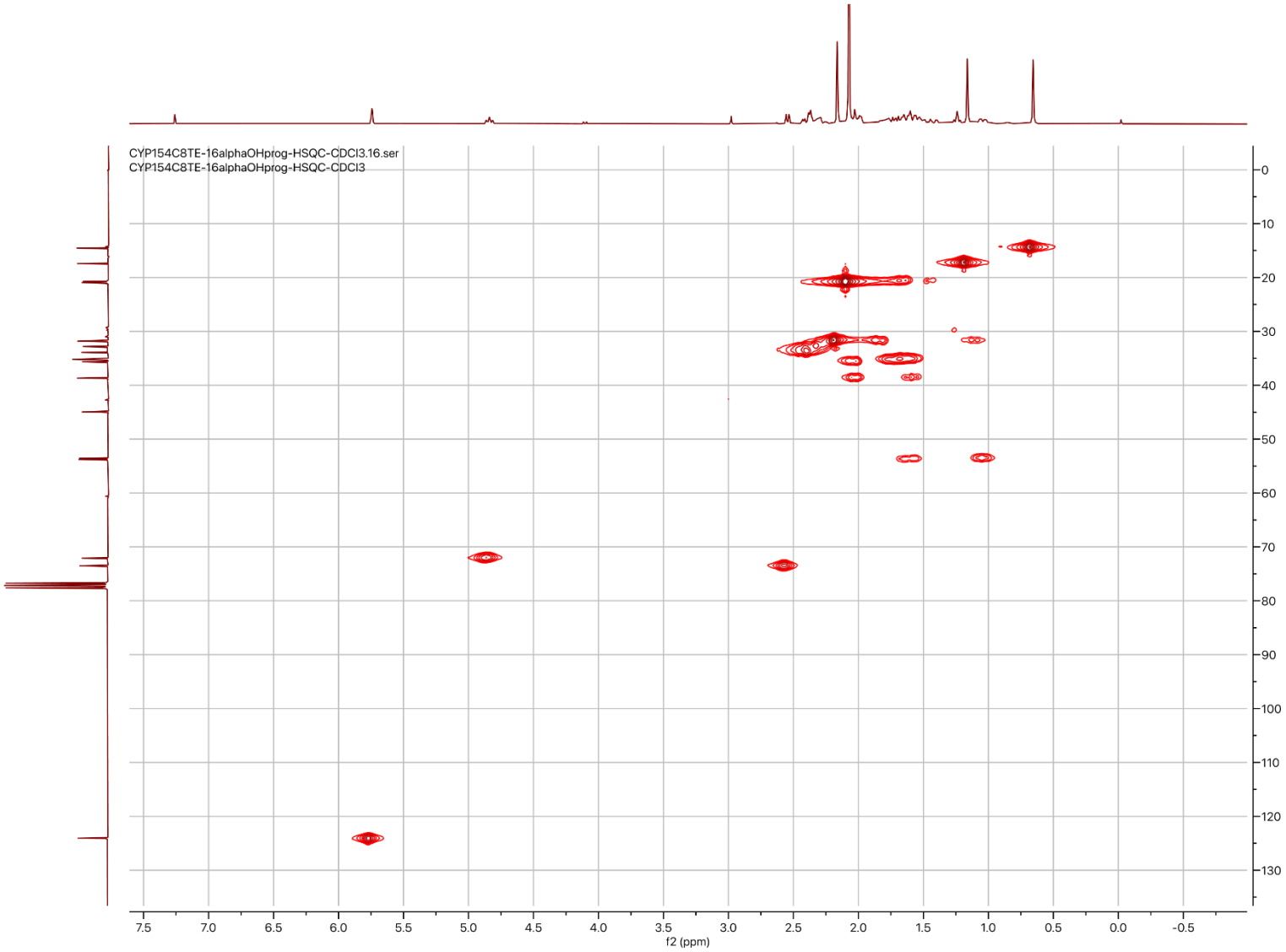
CYP154C8TE-16alphaOHprog-HSQC-CDCl3.16.ser
CYP154C8TE-16alphaOHprog-HSQC-CDCl3
0
10
20
30
40
50
60
70
80
90
100
110
120
130
7.5
7.0
6.5
6.0
5.5
5.0
4.5
4.0
3.5
3.0
2.5
2.0
1.5
1.0
0.5
0.0
-0.5
f2 (ppm)

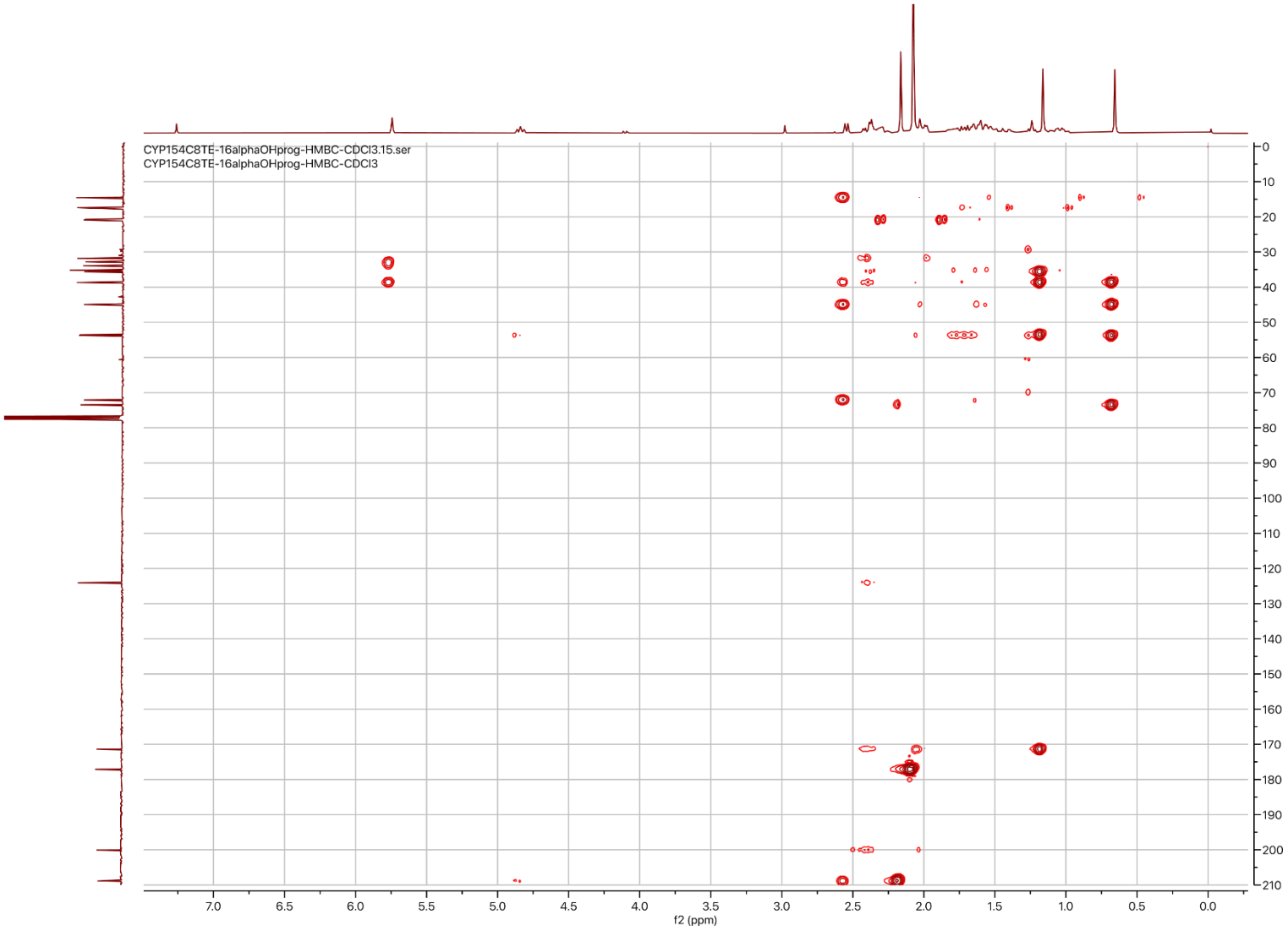
CYP154C8TE-16alphaOHprog-HMBC-CDCl3.15.ser
CYP154C8TE-16alphaOHprog-HMBC-CDCl3
f2 (ppm)

DNA sequences

Each sequence was cloned between the Nco I and Xho I resctriction sites of the pET28a vector (Twist Bioscience). Each contains a 6xHis tag and a Tobacco Etch Virus (TEV) cleavage site at the N-terminus and two stop codons and a Hind III site at the C-terminus.

CYP154C8 WT

GTGGCTCCAGCCATCACCATCACCATCACAGCAGCGGCGAAAACCTGTACTTCCAGGGCCATATGAATGGGCAAAGTG
CTACAACTTCAGCCGGCCAAGCCCCGGAGACAGGTCGCTGTCCATTAGTAATTGACCCGATGGTAGGCGACCTGGATG
GGGAAACGGCGGCGTTGCGCGAGGCAGCACCGATCACCCGCATCGATTTATTAGGGGTCCCTGCATGGACGGTGACA
AGCCATGCCGAGGCCCGTCGTTTGCTGAACGACAACCGTCTCGTTAAGGATATCAATCGTTGGGAGCTGTGGCGCAGT
GGCCAAGTCACGCACGAATGGCCATTAATCGGTATGATTGACGCAGGGCGTTCGATGTTCACAGTTGATGGCGCTGAG
CATCGTCGCCTTCGCGCGAAGACCGCACAGGCGGTAACCCCGCGCCGTCTGGAAGCACTCCGTCCGGTGATCGAGGAA
ATCACTGCACGCTTATTAGACGACTTGGCGGAGCGTGGCGCTGATGGTCCGGTGGACCTTAAACCAGTATTTGCACAAC
CGCTTCCTATGTTAGTGGTTAGCCACCTCATGGGAGTTGACCCGGCTTTACACCCCCGTCTGCATGAGCTCTACAAAGCC
TTCTTCAGCATGTTGACTCCCCAAGATGAACGCCTCGCAGTCATCGAGGAGCTGGACGTTATTTTCACCGAGATGGTTC
GCGAGCGTACCGCCGCGCCGGCGGATGATCTGACTAGCGCATTGATCCTGGCAGACGAGGGTGGGGAGCCGCTGACC
GAAGAAGAAGTAGTCGGGAATTTAAAGGCGATGGTTGCTGCCGGCCACGAGACTACGATCGGTCTCATCCTTAACGCT
GTTCGTGCATTGCTCACTCACCCGGACCAACTGGAGTTAGTTCTCGACGGGACCGTTGGTTGGGACACCGTGATCGAAG
AGACACTTCGCTGGGATACACCTACTACCCACTTGCTGATGCGCTTTGCGACTGAGGACATTCAGGTTGGCGACACTGT
AGTTCGCGAGGGTGAGGGAGTAGTCGTTTCCTACCGTGCCATCGGTCGTGATCGCGCCCAACACGGCGACGATGCAGA
CCGTTTTGATATCCGTCGTGAGACTCCTATTCGCCACATGACGTTCGGACACGGACCCCACATCTGTCCTGGTGCCGCAT
TATCGCGCCTGGAAGCTAGCATTGCACTGCCGGCGTTATTTGAACGTTTCCCTCGTCTGCGTTTGGCTGTTCCCGTGGAA
GAGATTCGCAACCTTCCTGTTTTAACCCAAAACGACCTGGCGGCATTCCCTGTCTTGCTGCACGGTAGTGGTGGTGGAA
GTATGCCTGGGCGCGCCCGCGCGCAGCGTCAAAGTAGCCGTGGCCGTTAATAAAAGCTT

CYP154C8 T258E

GTGGCTCCAGCCATCACCATCACCATCACAGCAGCGGCGAAAACCTGTACTTCCAGGGCCATATGAATGGCCAGTCCGC
CACGACGTCGGCCGGGCAAGCGCCAGAGACGGGACGCTGTCCGCTTGTAATCGATCCTATGGTTGGTGATCTGGATGG
TGAAACCGCCGCGCTTCGCGAAGCGGCACCGATCACGCGCATCGATCTTCTCGGGGTACCAGCATGGACTGTTACGAG
CCACGCCGAAGCGCGCCGTTTGTTGAATGACAACCGCCTCGTCAAAGACATTAATCGTTGGGAGCTGTGGCGCAGCGG
TCAGGTAACTCACGAGTGGCCTCTTATTGGCATGATTGACGCCGGTCGTTCAATGTTCACGGTCGATGGAGCTGAGCAC
CGTCGCTTACGTGCGAAGACCGCACAGGCGGTAACACCCCGCCGCCTGGAAGCCCTGCGTCCTGTAATTGAAGAAATC
ACGGCCCGTCTGTTAGATGACCTTGCGGAGCGCGGAGCGGATGGACCGGTAGATCTTAAGCCGGTTTTCGCACAGCCA
CTCCCCATGCTTGTGGTATCACATCTGATGGGAGTTGACCCGGCGTTACACCCTCGTTTACACGAGCTCTATAAGGCATT
CTTCAGTATGTTGACGCCTCAAGATGAGCGTCTGGCGGTAATTGAAGAGTTAGACGTGATCTTCACTGAGATGGTGCGT
GAACGCACAGCAGCCCCCGCAGACGACCTTACTTCAGCGCTCATCTTGGCCGATGAGGGTGGTGAGCCCTTAACTGAA
GAGGAAGTGGTGGGTAATTTAAAGGCGATGGTTGCGGCCGGACATgAGGAAACCATCGGCCTGATTCTTAACGCGGT
GCGTGCGCTCCTGACCCACCCCGACCAGCTGGAGCTGGTTCTCGATGGCACAGTGGGCTGGGACACCGTAATTGAAGA
AACCTTACGTTGGGACACCCCGACCACTCATCTCCTGATGCGCTTCGCGACCGAAGACATCCAAGTGGGTGATACCGTC
GTCCGCGAGGGTGAGGGTGTGGTTGTTAGCTACCGCGCAATCGGCCGTGACCGTGCACAGCATGGCGACGACGCCGA
TCGTTTTGACATCCGTCGCGAAACTCCAATCCGTCACATGACGTTCGGACACGGACCGCACATCTGTCCAGGTGCCGCC
CTCTCACGTCTGGAAGCATCAATTGCATTGCCTGCACTGTTTGAGCGTTTTCCACGCCTGCGCCTGGCGGTTCCAGTTGA
AGAAATCCGTAACTTACCTGTGCTGACGCAGAACGATTTAGCCGCTTTCCCAGTTTTGCTGCATGGATCAGGCGGTGGG
AGTATGCCTGGCCGCGCACGCGCGCAGCGTCAGAGTTCACGTGGTCGTTAATAAAAGCTT

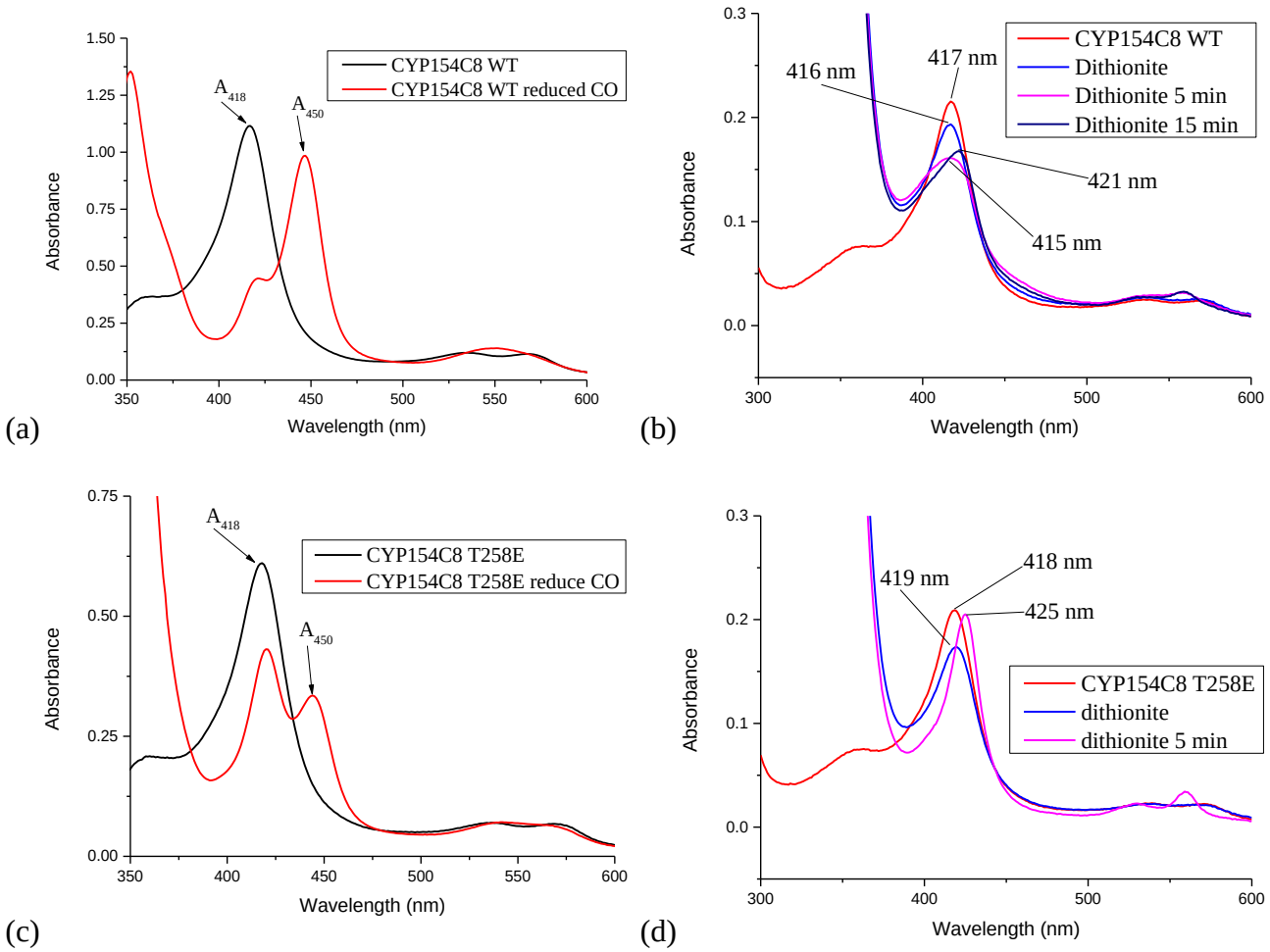

Figure S1 UV-visible absorbance spectra of the ferric (black) and ferrous-CO bound (red) forms of (a) WT CYP154C8 and (c) the T258E variant. Also included are the dithionite reduce UV-vis absorbance spectra of the WT enzyme (b) and the T258E mutant (d).

The ferrous spectra of the mutant and WT enzyme are different and both transition to another species over a 5-10 minute period. This is similar to recent observations with other P450 enzymes.[9]

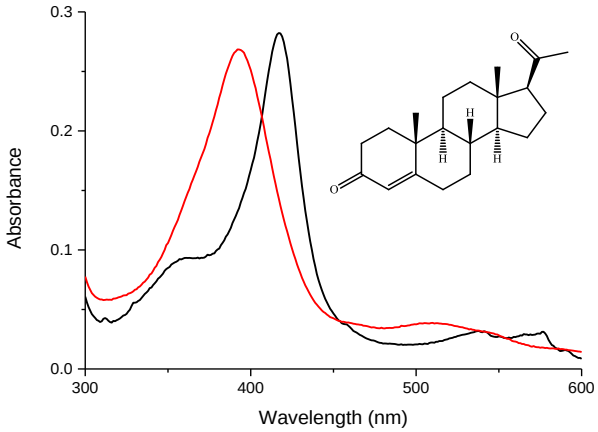

WT CYP154C8 with progesterone

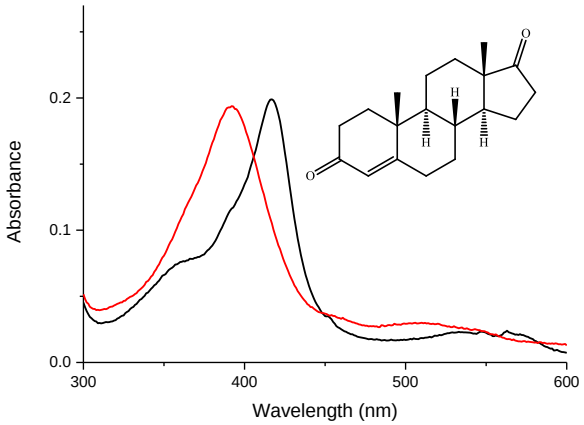

WT CYP154C8 with androstenedione

Figure S2 UV-visible absorbance spectra of the WT CYP154C8 before (black spectrum) and after (red spectrum) the addition of progesterone (top) and androstenedione (bottom).

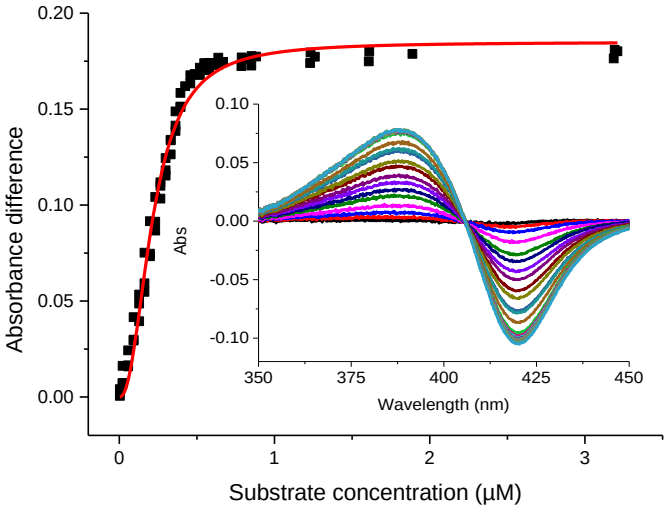

WT CYP154C8 and progesterone

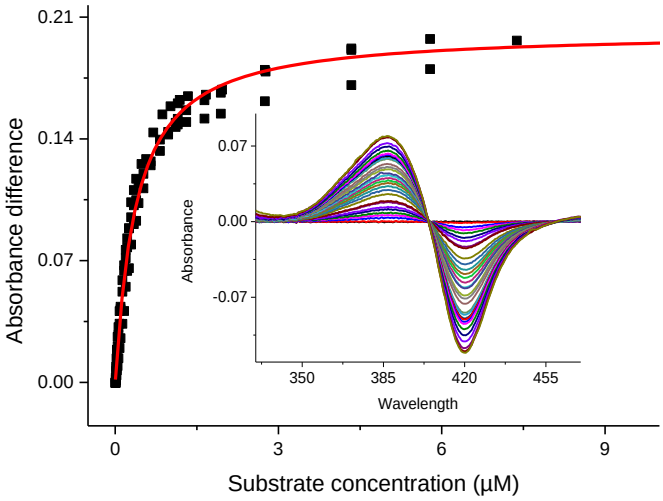

WT CYP154C8 and Androstenedione

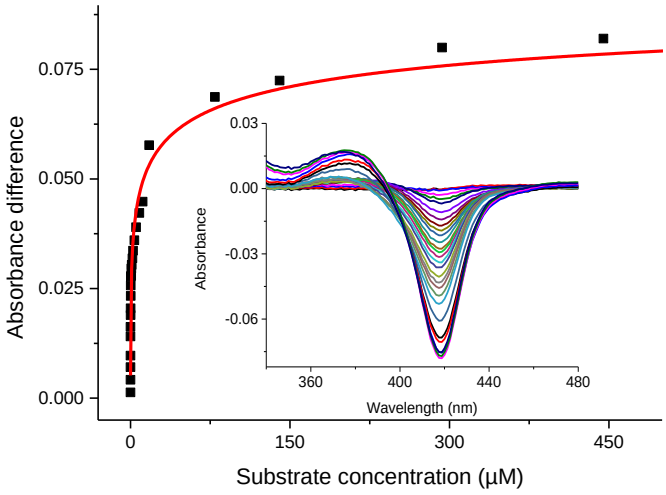

CYP154C8 T252E and androstenedione

Figure S3 Measurement of the binding affinity of progesterone and androstenedione for the WT and T258E variant of CYP154C8 using UV-visible spectroscopy.

Table S2 Dissociation constant analysis.

	T258E CYP154C8 Progesterone		T258E CYP154C8 Androstenedione	
	K_d	n	K_d	n
Hill Plot	0.37 ± 0.01	1.4 ± 0.04	13.1 ± 6.8	0.4 ± 0.03
	WT CYP154C8 Progesterone		WT CYP154C8 Androstenedione	
	K_d	n	K_d	n
Hill Plot	0.21 ± 0.01	2.3 ± 0.10	0.40 ± 0.02	1.0 ± 0.04

The fits were better with the Hill plot analysis when compared to simple hyperbola or a tight binding method (data not shown). All the methods showed similar trends and tight binding of the steroids to the CYP154C8 enzymes. Positive cooperativity was observed for progesterone binding. Androstenedione with the T258E mutant demonstrated negative cooperativity. The reason for the cooperativity effect are as yet are unclear. With the T258E mutant differences may be due to it being more difficult to displace the 6^{th} aqua ligand.

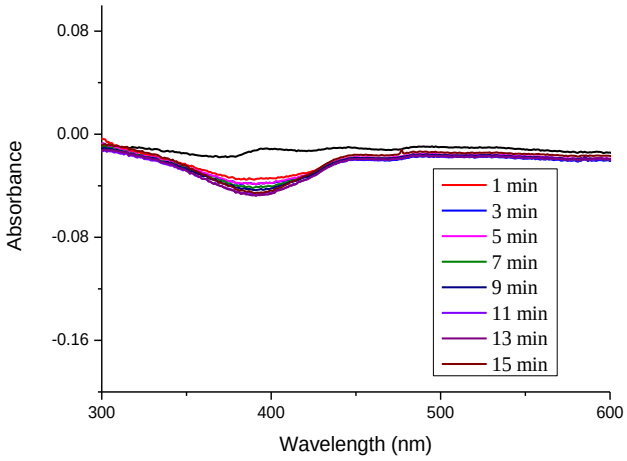

CYP154C8 T258E (2µM) and 200 µM progesterone with 20 mM H_2O_2

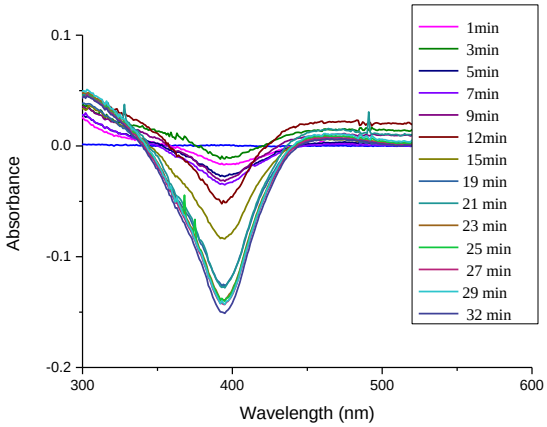

CYP154C8 T258E (2µM) and 200 µM progesterone with 30 mM H_2O_2

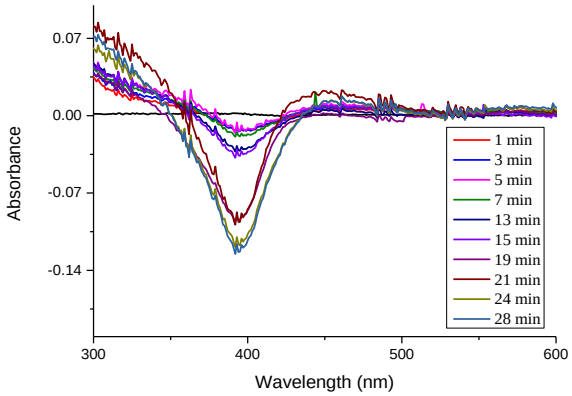

CYP154C8 T258E (2µM) and 200 µM progesterone with 40 mM H_2O_2

Figure S4. UV-visible absorbance spectra of the effect of different hydrogen peroxide concentrations on the heme of CYP154C8 T258E (2 µM) in the presence of progesterone (200 µM).

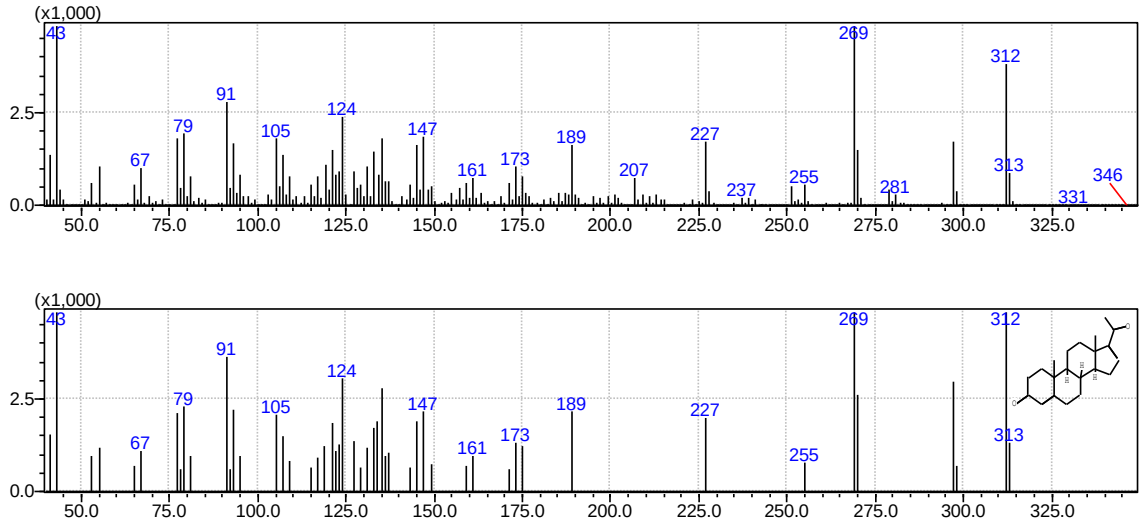

16α-hydroxyprogesterone, RT 18.9 min. Note the parent fragment of 16α-hydroxyprogesterone is not observed but peak at 312 (-18) is indicative of water elimination. The top spectrum is that obtained from the GC-MS analysis the spectrum below is that from the NIST library.

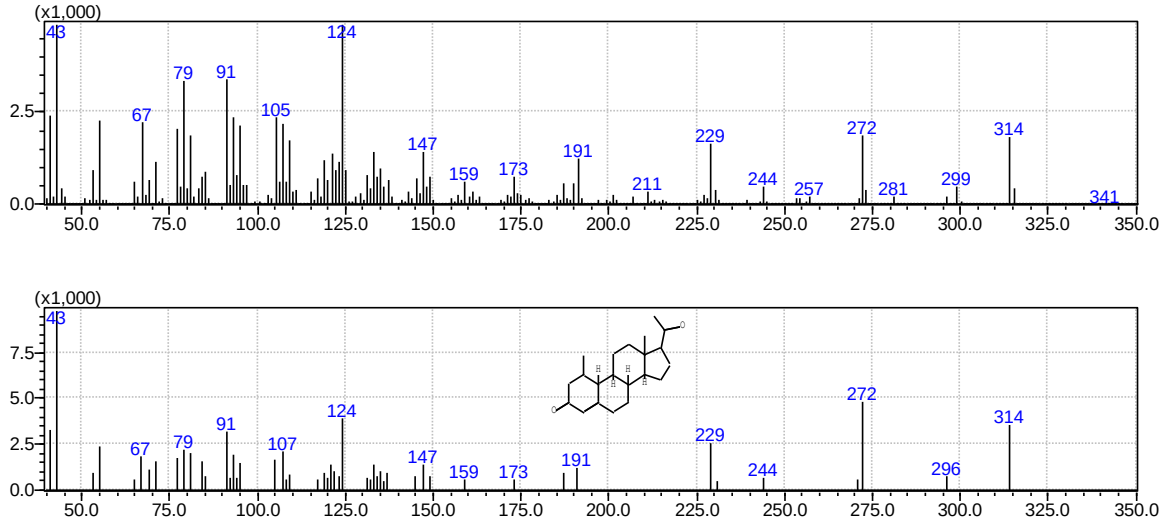

Progesterone, RT 19.3 min. The top spectrum is that obtained from the GC-MS analysis the spectrum below is that from the NIST library.

Figure S5. GC-MS analysis of the substrate and oxidation metabolite of progesterone by CYP154C8 T258E variant driven by hydrogen peroxide.

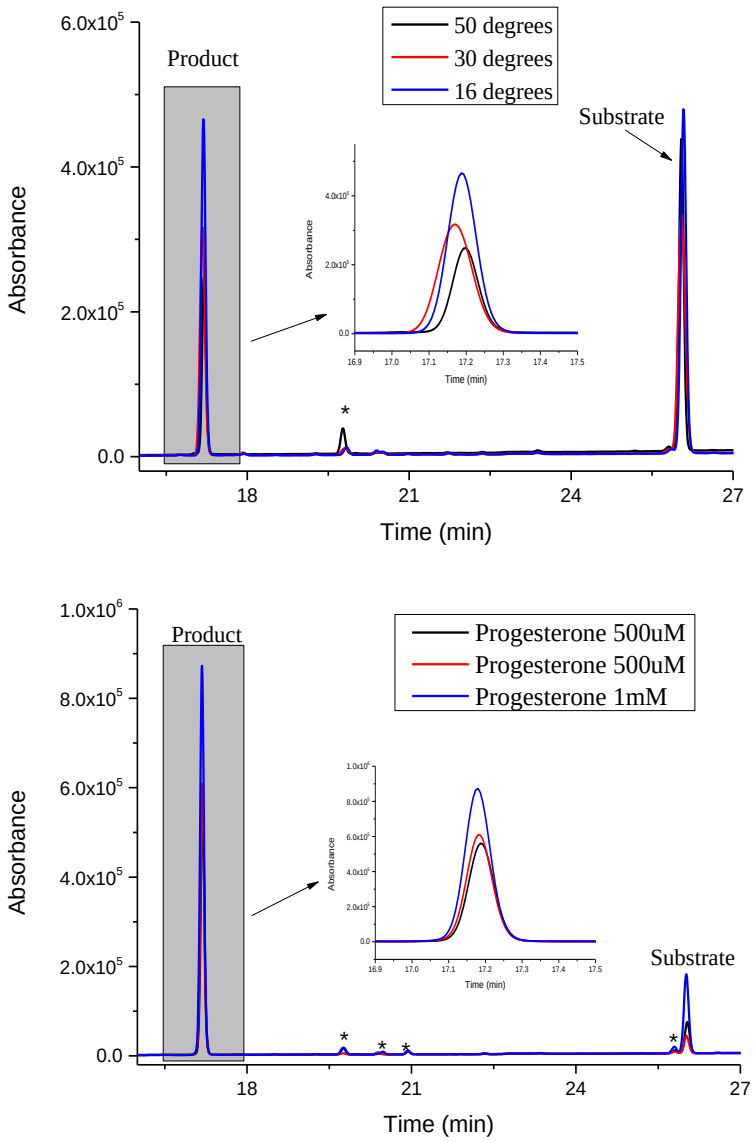

Figure S6. HPLC analysis of the conversion of progesterone to 16α-hydroxyprogesterone using the T258E variant of CYP154C8. The top chromatogram shows the conversion of progesterone (1 mM) at different temperatures (16 °C, 30 °C and 50 °C) by CYP154C8 T258E (1 µM) and 30 mM H_2O_2. The bottom chromatogram shows the conversion of 500 µM and 1 mM substrate using 1 µM enzyme and 20-40 mM H_2O_2.

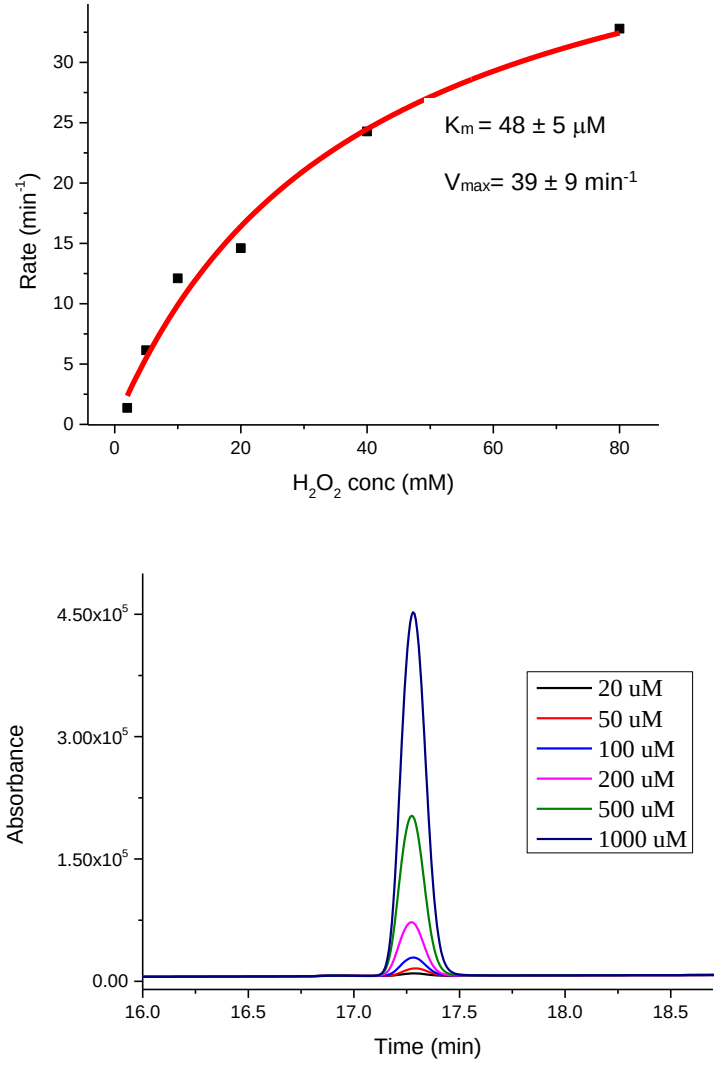

Figure S7. Variation of the rate of 16α-hydroxyprogesterone prodution using the T258E variant of CYP154C8 (1 μM) and progesterone (1 mM) by varying the H_2O_2 concentration (based on a 30 min reaction). The bottom chromatogram shows a calibration of the 16α-hydroxyprogesterone product versus the HPLC detector response.

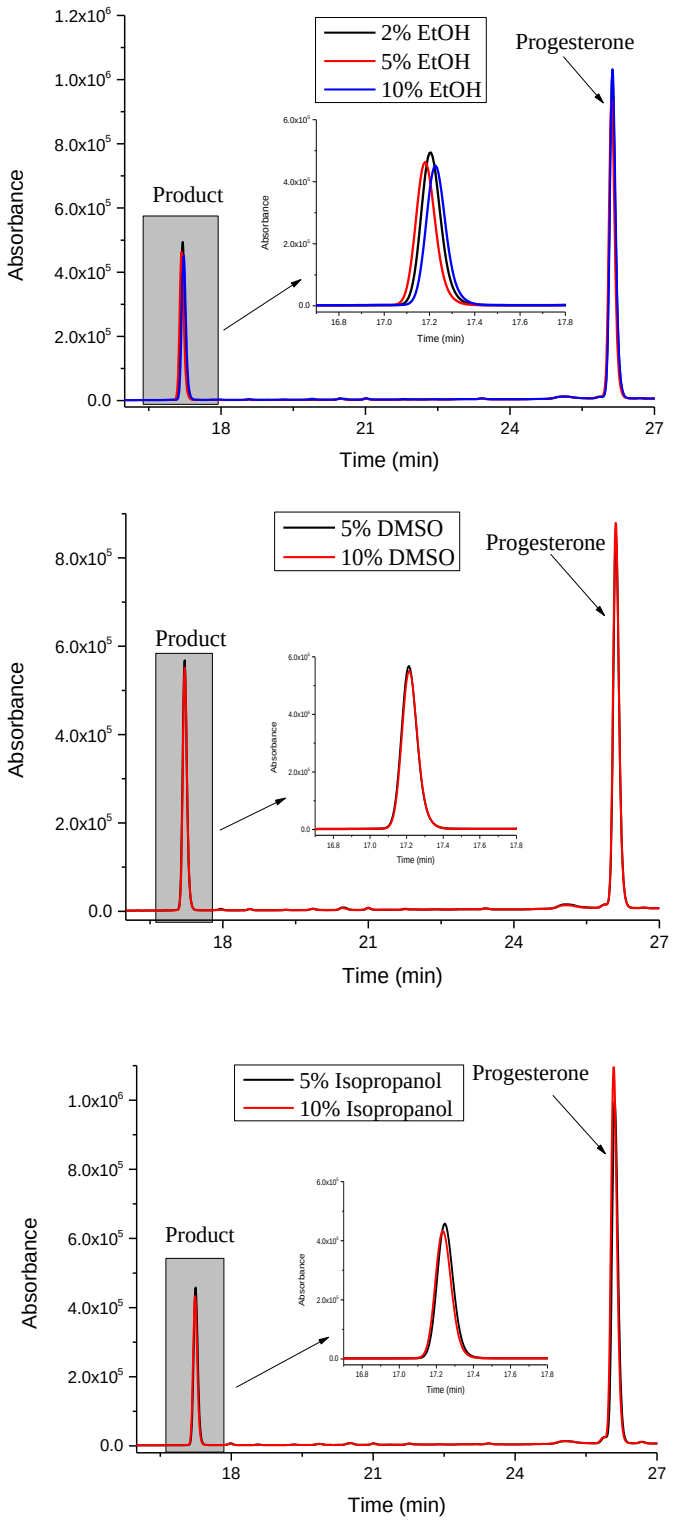

Figure S8. HPLC analysis of the conversion of progesterone (1 mM) to 16α-hydroxyprogesterone using the T258E variant of CYP154C8 (1 μM) using 20 mM H_2O_2 in the presence of 2%, 5% or 10% ethanol (EtOH), dimethylsulfoxide (DMSO) or isopropanol.

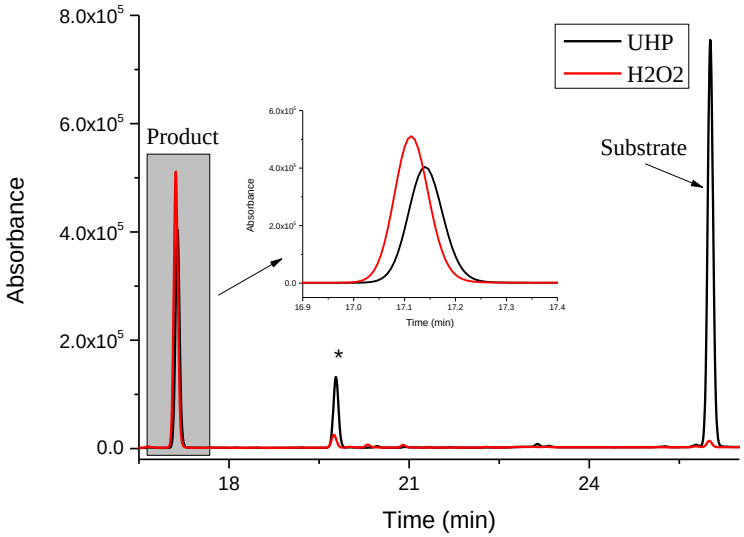

Figure S9. HPLC analysis of the conversion of progesterone (1 mM) to 16α-hydroxyprogesterone using the T258E variant of CYP154C8 (1 μM) using 30 mM H_2O_2 or urea-hydrogen peroxide (UHP).

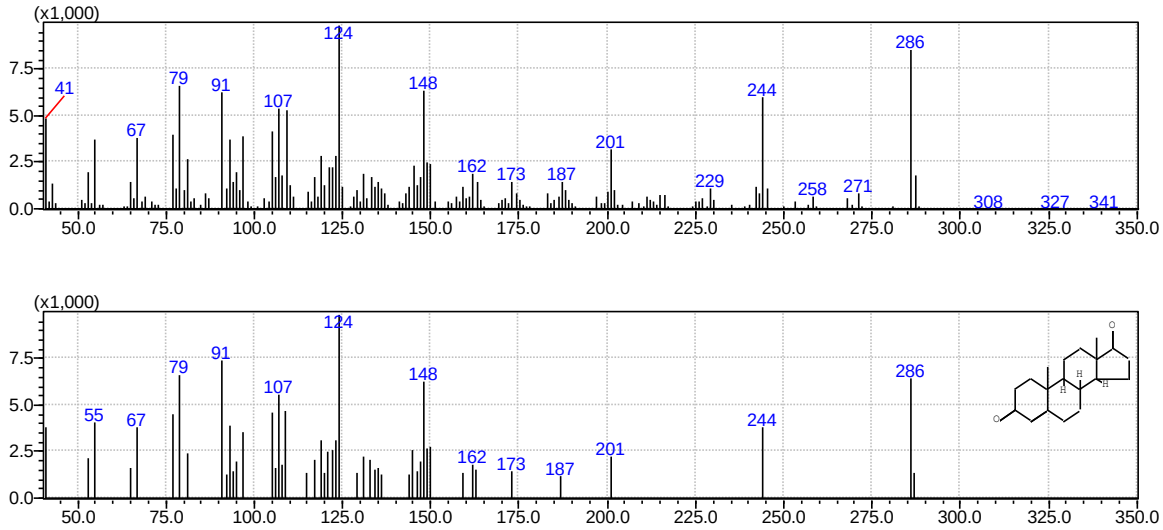

androstenedione RT The top spectrum is that obtained from the GC-MS analysis the spectrum below is that from the NIST library.

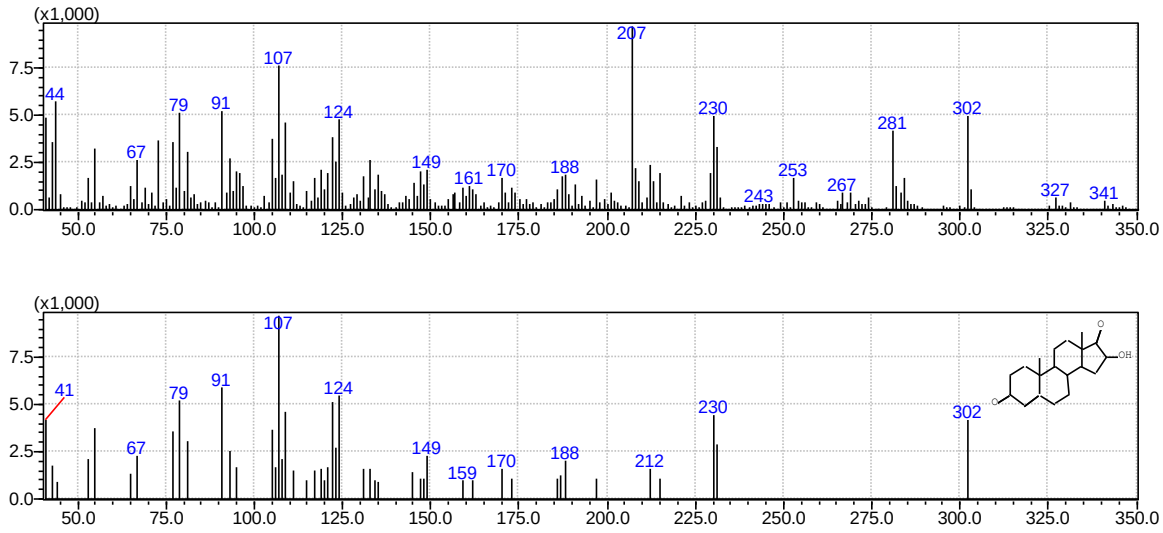

16α-hydroxyandrostenedione RT The top spectrum is that obtained from the GC-MS analysis the spectrum below is that from the NIST library. Note MS peaks from impurities on the GC-MS at 207, 253 and 281 are present.

Figure S10. GC-MS analysis of the substrate and oxidation metabolite of androstenedione by CYP154C8 T258E variant driven by hydrogen peroxide.

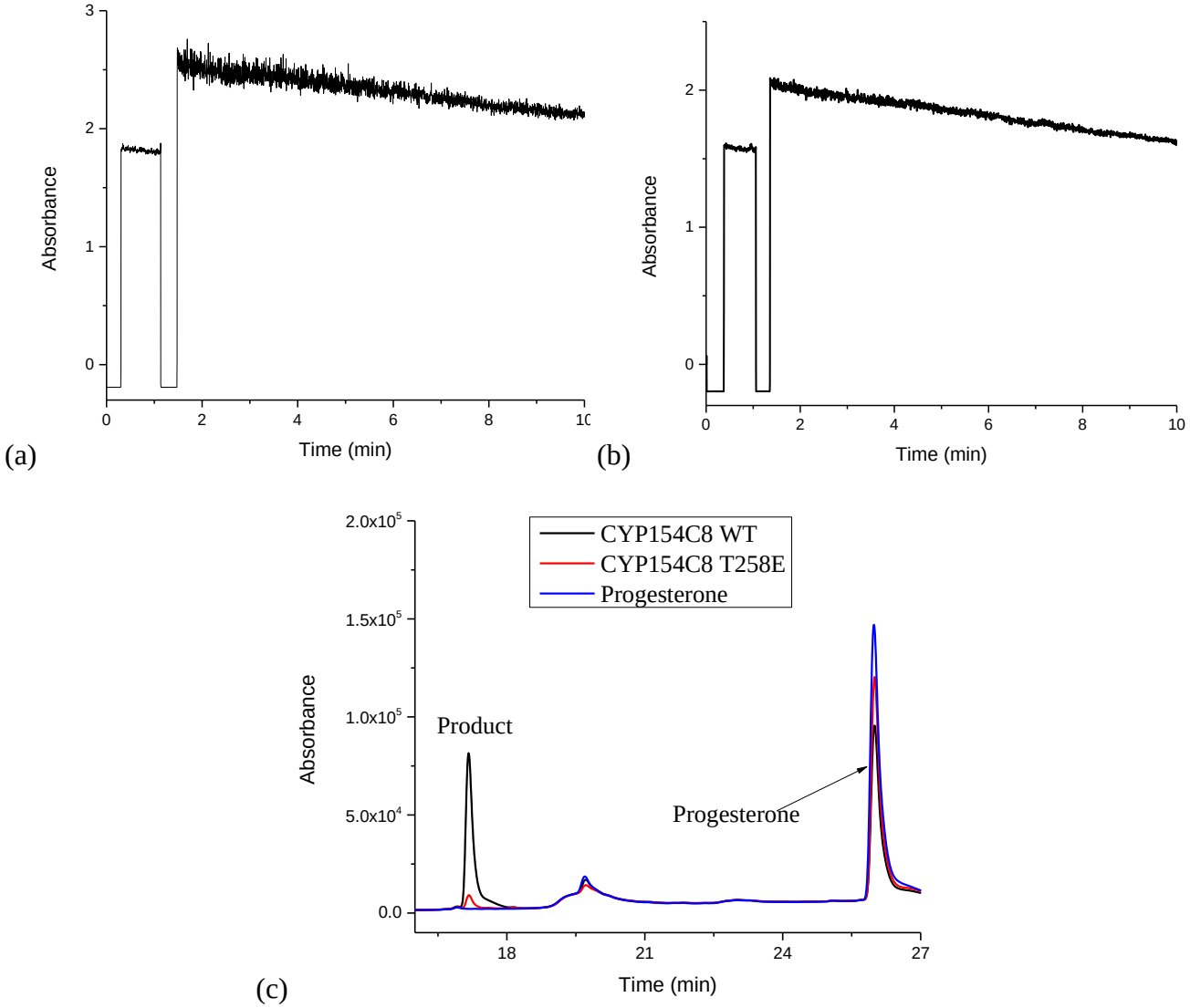

Figure S11 UV analysis of NADH oxidation by the (a) WT and (b) T258E mutant of CYP154C8. The reaction conditions were 1µM P450, 5 µM ferredoxin (HaPux) and 1 µM HaPuR (ferredoxin reductase) and 0.75 mM progesterone. Reactions were commenced by the addition of 250 µM NADH (c) The HPLC analysis of the monooxygenase turnovers of each mutant demonstrating the reduced activity of the T258E mutant of CYP154C8. The WT enzyme generated approximately 10-fold more product than the T258E mutant (relative to the amount of NADH added).

Note when the alternative electron transfer partners spinach ferredoxin and spinach ferredoxin reductase were used with CYP154C8 either WT or the T258E mutant little or no product was formed. Therefore, the HaPuR/HaPux system maybe promising for whole-cell oxidation studies with CYP154C8.[10]

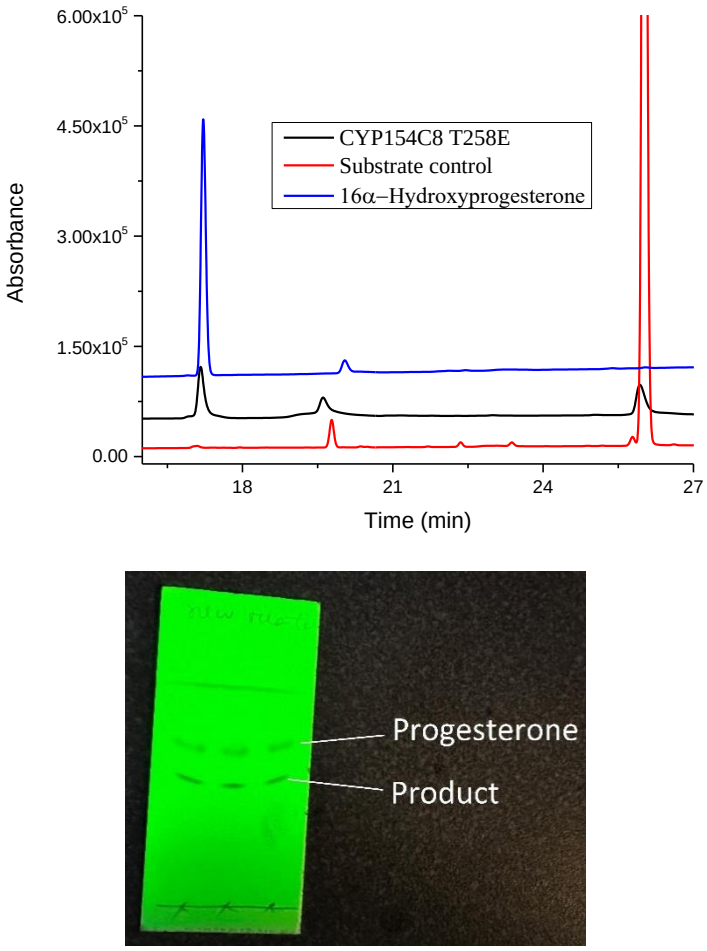

Figure S12 (a) TLC and HPLC monitoring of the large scale (100 mL) reaction CYP154C8 T258E reaction with progesterone (1 mM) and 40 mM H_2O_2 (reaction on the left and substrate control on the right).

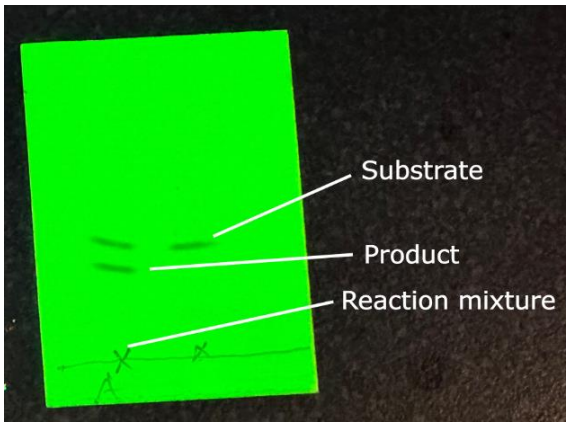

Figure S12 (b) TLC of monitoring of the large scale reaction CYP154C8 T258E reaction with androstenedione (1 mM) and 40 mM H_2O_2 (reaction on the left and substrate control on the right).

References

1. T. Omura and R. Sato, *J Biol Chem*, 1964, **239**, 2370-2378.
2. T. C. Pochapsky, N. Wong, Y. Zhuang, J. Futcher, M.-E. Pandelia, D. R. Teitz and A. M. Colthart, *Biochim Biophys Acta Proteins Proteom*, 2018, **1866**, 126-133.
3. K. P. Conner, C. M. Woods and W. M. Atkins, *Arch Biochem Biophys*, 2011, **507**, 56-65.
4. S. G. Bell, R. Zhou, W. Yang, A. B. Tan, A. S. Gentleman, L. L. Wong and W. Zhou, *Chemistry–A European Journal*, 2012, **18**, 16677-16688.
5. J. S. Harbort, J. J. De Voss, J. E. Stok, S. G. Bell and J. R. Harmer, *Future directions in metalloprotein and metalloenzyme research*, 2017, 103-142.
6. F. P. Guengerich, C.-H. Yun and T. L. Macdonald, *J Biol Chem*, 1996, **271**, 27321-27329.
7. J. M. Hutzler, F. J. Powers, M. A. Wynalda and L. C. Wienkers, *Arch Biochem Biophys*, 2003, **417**, 165-175.
8. B. Dangi, K. H. Kim, S. H. Kang and T. J. Oh, *Chembiochem*, 2018, **19**, 1066-1077.
9. H. Mohamed, A. Ghith and S. G. Bell, *J Inorg Biochem*, 2023, **242**, 112168.
10. S. G. Bell, A. B. Tan, E. O. Johnson and L. L. Wong, *Mol Biosyst*, 2010, **6**, 206-214.